

# Observations of the spectral variability of $\epsilon$ Cephei

S. Pokhvala, B. Zhilyaev

Main Astronomical Observatory of National Academy of Sciences of Ukraine, Kyiv  
nightspirit10@gmail.com

(Research report. Submitted on 01 May 2025; Accepted on 25 June 2025)

**Abstract.** We report the results of observations of small-scale variability in the Balmer lines of hydrogen in the spectrum of  $\epsilon$  Cephei. Spectral observations were conducted using a low-resolution spectrograph ( $R \simeq 600$ ). The spectra were obtained with a time resolution of 5.79 s. It is found that  $\epsilon$  Cephei exhibits variations in the hydrogen lines  $H_\beta$ ,  $H_\gamma$ ,  $H_\delta$ ,  $H_\epsilon$ . Discrete frequencies of about 3 mHz are observed in  $\epsilon$  Cephei, similar to the five-minute oscillations excited by p-modes in the Sun. The characteristic time of the observed oscillations ranges from 337 s. The horizontal scale for the oscillations is about 125 Mm. The radial velocity of the variations is about  $180 \text{ km s}^{-1}$ .

**Key words:** instrumentation: detectors – methods: observational – techniques: image – stars:  $\epsilon$  Cephei

## Introduction

$\epsilon$  Cephei is an F-type star with a stellar classification of F0 V (Gray et al. 2001) or F0 IV (Mawet et al. 2011). It may either be an F-type main sequence star, or it could be a more evolved subgiant star. It is a  $\delta$  Scuti variable star that cycles between magnitudes 4.15 and 4.21 every 59.388 minutes (AAVSO).

Asteroseismology of the  $\delta$  Scuti star  $\epsilon$  Cephei was carried out with the WIRE satellite, combining ground-based and space-based photometry (Bruntt et al. 2006).

The ground-based data set consists of 16 nights of data collected over 164 days, while the satellite data provide a nearly continuous coverage of the star during 14 days. The authors detect 26 oscillation frequencies in the WIRE data set, but only some of these can be seen clearly in the ground-based data. The authors used multicolor ground-based photometry to determine amplitude and phase differences in Stromgren filters in an attempt to determine the radial extent of the oscillation frequencies. They concluded that the accuracy of the amplitudes and phases is insufficient to constrain the theoretical models of  $\epsilon$  Cephei. They find no evidence of rotational splitting or large separation between the frequencies found in the WIRE dataset.

To be able to identify oscillation frequencies in  $\delta$  Scuti stars, it is crucial to obtain a more complete coverage from multi-site campaigns with a long time baseline.

Bruntt et al. (2006) analyzed periods in the range of 0.7-1.9 hours, which is typical for stars with low  $\delta$  Scuti amplitudes. They analyzed  $\epsilon$  Cephei models with modes of spherical harmonics inherent in "global oscillations". Amplitude ratios and phase differences were calculated for  $l = 0, 1$ , and 2. This is peculiar for g-mode oscillations with periods close to the fundamental radial mode.

In our work, we combined ground-based photometry of  $\epsilon$  Cephei with spectral observations made on an Alpy 600 spectrograph. Spectral observations allow us to find evidence of rotational splitting and determine the radial frequencies of oscillations. The amplitudes and phases of the harmonics will enable us to construct a theoretical model of  $\epsilon$  Cephei.

If  $\epsilon$  Cephei is variable, what is the expected time scale? As a basis for discussion, we shall consider the fundamental period of radial oscillation. This is determined almost entirely by the star's mass and radius, which can be derived reliably in a well-studied star like  $\epsilon$  Cephei. A model with mass  $M/M_{\odot} = 1.65$  (Trevor and Lynne 2015),  $R/R_{\odot} = 1.86$  (Rhee 2007), and  $T_e = 7720$  K (Trevor and Lynne 2015) was used.

The period of the fundamental radial pulsation can be calculated from the relation  $P\sqrt{\rho} = Q$ , where  $\rho$  denotes the mean stellar density.  $Q$  is a function of  $M_*/R_*$ . Kogan (1970) created models whose range of masses and radii includes  $\epsilon$  Cephei. It is  $Q = 0.0335 \pm 0.0005$  days. Given this value and the mass and radius, the pulsation period  $P = 0.056 \pm 0.03$  days can be predicted.

Given the values of rotation rate  $91 \pm 10$  km s $^{-1}$  (Royer et al. 2006) and radius, we can predict a rotation period of 1.04 days.

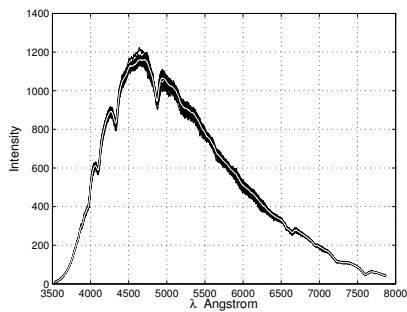


**Fig. 1.** The spectra of  $\epsilon$  Cephei.

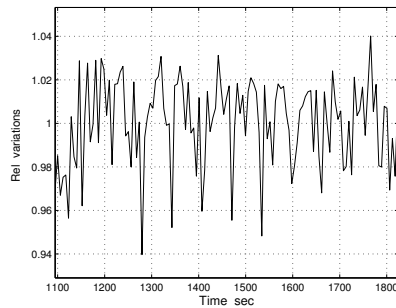


**Fig. 2.** Variations of intensity of  $\epsilon$  Cephei in the V band.

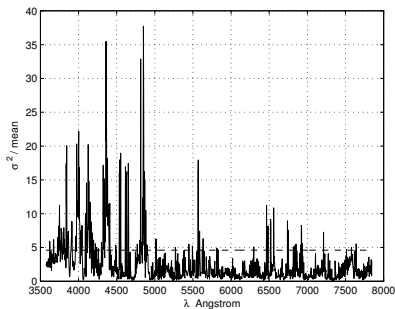


**Fig. 3.** Variations in the spectrum of  $\epsilon$  Cephei.

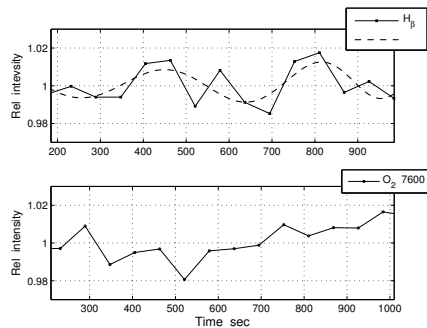


**Fig. 4.** Light curves in the  $H_{\beta}$  4861 Å line (upper panel), and atmospheric oxygen line  $\lambda$  7600 Å.

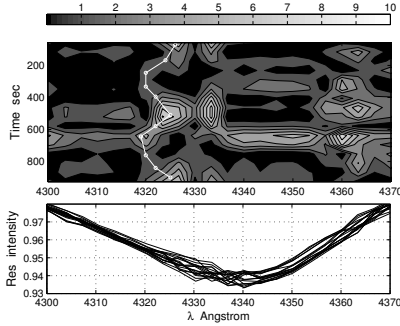
## Observations

Spectral observations of  $\epsilon$  Cep (HD 211336) were carried out at the Main Astronomical Observatory with the Schmidt-Cassegrain 6-inch Intes-Alter M603 telescope in 2024 August 24. The purpose of the observations was to obtain spectra of the star to study the rapid variability of spectral lines. To study the spectral variability of  $\epsilon$  Cep, spectra were obtained with an Alpy 600 spectrograph with an effective resolution of  $3.22 \text{ \AA}$  in the wavelength range  $3500 - 7800 \text{ \AA}$ . The time resolution was  $5.79 \text{ sec}$ . 380 spectra were obtained for a time interval of  $2200 \text{ sec}$ . The Schmidt-Cassegrain 6-inch f/6.4 Intes-Alter telescope M603 provides a signal-to-noise ratio of 10 for the program star.

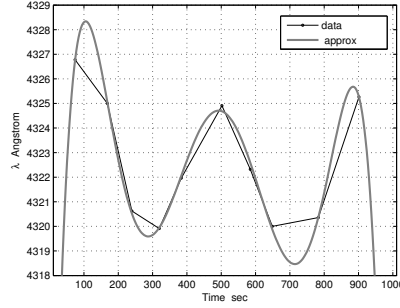
Combined ground-based photometry of  $\epsilon$  Cep was performed with V-measurements on the C11 telescope. The data were collected in 2024 September 24. 200 measurements were obtained with a temporal resolution of  $60.80 \text{ sec}$ .

Fig. 1 shows recorded spectra of  $\epsilon$  Cep. Fig. 2 shows variations of intensity of  $\epsilon$  Cep in the V band.

## The detection of line-profile variations



**Fig. 5.** Dynamic spectrum of the  $H_\gamma$  4340  $\text{\AA}$  line (upper panel). SNR versus time. Residual line intensity (lower panel).



**Fig. 6.** Variations of radial velocity in the center of line  $H_\gamma$ .

The following Fig. 3 shows the dependence of the variance on the mean intensity in the spectrum of the star. For Poisson random variables, the following relation holds (Pollard 1979):

$$(n - 1) \sigma^2 / \text{mean} = \chi_{V,n}^2,$$

where  $\sigma$  is the variance,  $n$  is the number of measurements.  $\chi_{V,n}^2$  is the inverse of the chi-square cumulative distribution with  $n$  degrees of freedom at the values in  $V$ .

The formula allows setting a detection threshold. For  $n = 18$  the 90% detection threshold for relative variations is 4.61.

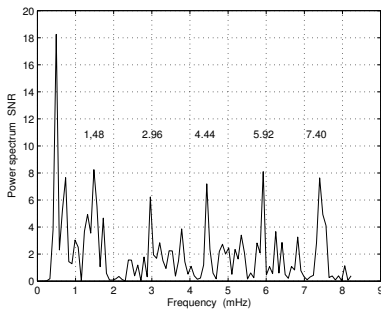
In Fig. 3 one can see activity in the hydrogen lines  $H_\xi$ ,  $H_\delta$ ,  $H_\gamma$ ,  $H_\beta$ , and atmospheric lines of oxygen ( $\lambda$  6870 Å and  $\lambda$  7600 Å) and water ( $\lambda$  7180 Å).

Figure 4 shows the light curves of the  $H_\beta$  4861 Å line and the atmospheric oxygen  $\lambda$  7600 Å line. It is easy to see a harmonic with a period of about 337 seconds and an amplitude of about 0.01 stellar magnitude.

Line profile variations are a very valuable diagnostic to detect both radial and non-radial oscillations (e.g. Aerts et al. 2003, and references therein; Hekker et al. 2006), and to characterize the wave numbers ( $l, m$ ) of such self-excited oscillations. It is worthwhile to detect them for  $\epsilon$  Cep with confirmed oscillations and to use them for empirical mode identification.

The dynamic spectrum in Fig. 5 demonstrates the change of  $H_\gamma$ , showing the signal-to-noise line profiles as a function of time.

Fig. 6 shows the  $\lambda$ -scale variations of the radial velocity in the  $H_\gamma$  line from the dynamic spectrum in Fig. 5.



**Fig. 7.** Fourier spectrum of the light curve of  $\epsilon$  Cep.

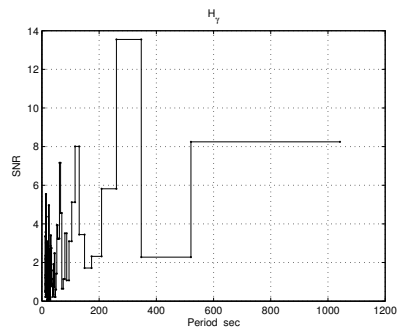


**Fig. 8.** Fourier spectrum of the  $H_\gamma$  line light curve of  $\epsilon$  Cep.

## Restoration of spectral line activity

To analyze the line profile variations in the spectrum of a star, we use the technique developed in Fullerton et al. (1996) for absorption lines in O stars. As a result of the observations, each spectral time series can be represented by a two-dimensional array  $S$ . Each element of the matrix  $S_x$  represents the wavelength of the spectrum in the time series. The row  $S_y$  of the matrix highlights the entire spectral wavelength band at one point in time, while each column tracks the behavior of a single wavelength as a function of time. This data representation is visualized in Figure 5.

Qualitative analysis of spectrometric data consists of identifying peaks and estimating their position and intensity. Deconvolution methods are an effective tool for peak detection and estimation.

To estimate the dynamical spectrum of the nonradial oscillations, we use the technique of polarization estimation through an integral function called Zeeman signature (Donati et al. 1997). The Zeeman effect splits spectral lines in the presence of a magnetic field. In our case, the rotation of the star splits the modes of nonradial oscillations. The Zeeman signature technique increases the resolution in spectrum analysis.

The new spectrum estimate obeys the expression

$$I_{loc} = \left| \frac{\partial^2 I}{\partial^2 \lambda} \right|,$$

where  $I$  is the profile of the spectral line and  $\lambda$  is the wavelength. If the line profile is approximated by a Gaussian curve, this transformation preserves the line profile and increases the signal-to-noise.

The formula below deconvolves an image  $I$  using the maximum likelihood algorithm and an initial estimate of the point-spread function PSF (Morhac and Matousek 2011)

$$I_\lambda = \int PSF \cdot I_{loc}(\lambda - \lambda_c) \cdot \partial \lambda_c.$$

We use the Richardson-Lucy algorithm. It uses a statistical model to generate the data and is based on Bayes formula. This iterative method forces the deconvolved spectra to be non-negative. The Richardson-Lucy iteration converges to a maximum likelihood solution for Poisson statistics in the data.

The image in Fig. 5 shows the restoration of the oscillation spectrum in the  $H_\gamma$  4340 Å line after 200 iterations. We used a Gaussian model for the PSF peaks.

Figure 6 shows the temporal changes in the line profile after recovery. In Fig. 6 the period of variations is about 337 seconds (5.6 min), and the amplitude is about  $3 \pm 1$  Å. These quantities characterize the variations of the line profile in the observer's coordinate system.

## Results and conclusions

Figure 7 shows the power spectra of  $\epsilon$  Cep in signal-to-noise (SNR) – frequency coordinates in mHz. In a series with a duration of 1200 seconds, several harmonics with equal spacing in frequency of 1.48 mHz are observed.

The Fourier spectrum of the light curve of the  $H_\gamma$  line (Fig. 8) shows a harmonic with a frequency of 2.96 mHz (a period of 337 s).

Warner and Robinson (1972) assumed the equal spacing in frequency to be due to the rotational splitting of nonradial modes.

The theory predicts that the visible stellar layers are driven by a set of standing waves, each covering the whole surface, and having a radial velocity  $V$  whose temporal and spatial dependence is given by

$$V \sim \sin(\sigma \cdot t) \cdot Y_m^l(\theta, \phi),$$

where  $Y_m^l(\theta, \phi)$  denotes the spherical harmonics,  $\theta$  the colatitude, and  $\phi$  the azimuth angle in the spherical coordinate,  $\sigma$  the frequency, and  $t$  – time (Unno et al. 1979).

The nonradial mode of oscillations of the spherical harmonics with quantum numbers  $k, l, m$ , where  $m$  are the integers in the range  $(-l, \dots, 0, \dots, l)$ , for stars with angular rotational velocity  $\Omega$  has the following form

$$\sigma = \sigma_0 + 2 \cdot m \cdot \Omega \cdot C_{k,l},$$

where  $\sigma_0$  is the mode frequency in the absence of rotation,  $C_{k,l}$  is a constant depending on the structure of the star. The constant  $C_{k,l}$  is suggested by Ledoux (1951). For the homogeneous model it is equal to unity. Then the frequency splitting has the form (Deubner 1977):

$$\Delta\sigma = 2 \cdot |m| \cdot \Omega.$$

Acoustic p-modes exhibit high-frequency oscillations with a period of 337 sec. For a rotational period of 1.04 days and  $\Delta\sigma = 2 \cdot \pi/337$  Hz, we obtain an estimate of the azimuthal number  $m \simeq 65$ .

Horizontal wavelengths can be provided, respectively, by eigenmodes  $l$  and  $m \simeq 65$ , in which large amplitude spots appear to have average sizes of about 125 Mm for  $\epsilon$  Cep. Note that the horizontal scale for oscillating features for the Sun is between 10 and 30 Mm (Musman and Rust 1970).

The radial velocity  $V$  according to Fig. 6 is about 3 Å, which corresponds to 180 km s<sup>-1</sup>.

The present work solves the problem of searching for the intrinsic variability of spectral lines of  $\epsilon$  Cep.

Dynamic spectroscopy of  $\epsilon$  Cep using a spectrograph with a spectral resolution of  $R \sim 600$  allowed us to detect rapid variations in the hydrogen lines. The characteristic time of the observed oscillations is 337 s (5.6 min).

The horizontal scale for oscillating elements is about 125 Mm. The radial velocity of the variations is about 180 km s<sup>-1</sup>.

$\epsilon$  Cephei exhibits discrete frequencies around 3 mHz, similar to the five-minute oscillations excited by p-modes on the Sun.

## References

- Aerts, C., and De Cat, P., 2003, *Space Science Reviews*, 105, 453  
 Bruntt, H., Suarez, J.C., Bedding, T.R., et al., 2006, arXiv:astro-ph/0610539v1 18 Oct 2006  
 Deubner, F.L., 1977, *Bull. American Astron. Soc.*, 9, 375  
 Donati, J.F., Semel, M., Carter, B.D., et al., 1997, *MNRAS*, 291, 658-682  
 Fullerton, A.W., Gies, D.R., and Bolton, C.T., 1996, *ApJS*, 103, 457-512  
 Gray, R.O., Napier, M.G., and Winkler, L.I., 2001, *AJ*, 121 (4): 2148-2158  
 Hekker, S., Aerts, C., De Ridder, and Carrier, F., 2006, arXiv:astro-ph/0608452v1 21 Aug 2006  
 Kogan, B.C., 1970, *ApJ*, 162, 139  
 Ledoux, P., 1951, *ApJ*, 105, 305  
 Mawet, D., Mennesson, B., Serabyn, E., et al., 2011, *The Astrophysical Journal Letters*, 738, 1, L12, 5 pp.  
 Morhac, M., and Matousek, V., 2011, *Journal of Computational and Applied Mathematics* 235, 1629-1640  
 Musman, S., and Rust, D.M., 1970, *Solar Phys.*, 13, 261  
 Pollard, J.H., 1979, *A handbook of numerical and statistical techniques*, Cambridge University Press, Cambridge  
 Rhee, J.H., 2007, *ApJ*, 660 (2): 1556-1571  
 Royer, F., Zorec, J., and Gomez, A.E., 2006, arXiv:astro-ph/0610785v1 26 Oct 2006

Trevor, D., and Lynne, H., 2015, ApJ, 804 (2): 146

Unno, W., Osaki, Y., Ando, H., and Shibahashi, H., 1979, Nonradial Oscillations of Stars,  
University of Tokyo Press

Warner, B., and Robinson, E.L., 1972, Nature, Phys. Sci., 239, 2